Effect of Inhomogeneous Distribution of Alloying Elements on Integrity of Al-2.1 wt.% Mg Alloy Tubes and Welds

Gargi Choudhuri, R Pal, P Nanekar, D Mukherjee
Quality Assurance Division, Bhabha Atomic research Centre, Mumbai, India 400085
E-mail: gargi@barc.gov.in

Abstract: Al-2.1 wt.% Mg alloy is an important nuclear research reactor material. The tubular products of the alloy are usually made by port-hole die extrusion process and several quality control steps are involved during fabrication to assess the quality of the weld joint. The paper describe two cases of failures of the alloy during fabrication. In one case, a thin wall tube failed during hydro-test at the weld-line while in another, a through-wall crack is observed at the heat affected zone (HAZ) of the weld joint between the thin tube and the tie-plate. In both the cases, the fracture surfaces have the appearance of brittle failure without any gross plastic deformation. Visual inspection, liquid penetrant testing, optical microscopy (OM), scanning electron microscopy (SEM) with energy dispersive spectrometry (EDS), Electron back scattered diffraction (EBSD) and micro-hardness measurement have been carried out for root cause analysis of the failures. EDS analysis at low KV indicates high Magnesium (Mg) and Silicon (Si) content at the fracture surface in both the cases. In the first case, segregation of these alloying elements at the weld-line in the port hole extruded tube has been observed. In the second case, the microstructure at the HAZ location shows grain boundary precipitation of low melting phase containing Mg, Si and Fe. Presence of Mg and Si reduce the solidus temperature of the grain boundary phase, which is responsible for HAZ liquation leading to failure under tensile stress during cooling.
Keywords*:* Al-Mg alloy; Port hole die extrusion; HAZ liquation; Low melting phase

1. Introduction

Al-2.1 wt.% Mg alloy is a work-hardenable material with moderate to high strength. This alloy is widely used in automobile industry, nuclear research reactors, marine industry and cryogenic application. The tubes of this alloy are fabricated through the port-hole die extrusion process. The extrusion is followed by a number of cold drawing steps and intermediate annealing to achieve the required dimensions, microstructure and mechanical properties. During port-hole extrusion process [1, 2], the alloy is allowed to flow through port-holes around the core support that holds the stationary mandrel. The metal streams flowing through the port holes join in the chamber prior to their exit from the die. The most critical aspect in this process is the satisfactory joining of all the streams, which is dependent on the pressure distribution in the welding plane [3-6]. Factors such as die design, extrusion ratio, extrusion speed and billet temperature affects the joining process [7-15]. Another concern of the port hole die extrusion is the metal flow from billet surface or sub surface region having oxide or any other type of contamination, into the welding region, resulting in poor weld joint with oxide band and segregation [2]. The joining of the streams is the solid state bonding process without the formation of liquid phase. The quality of the joint is assessed by visual inspection, tensile testing and hydro-test. If the joint is not proper, the tube may open up along the seam during further processing [16].

Another important issue during fabrication of Al-Mg alloy is the solidification cracking or liquation cracking due to presence of low melting intermetallics [17-19]. For Al-Mg system, Al_3Mg_2 (around 35 to 39 wt.% Mg) and $Al_{12}Mg_{17}$(42 to 58 wt.% Mg) are the two low melting intermetallic phases with eutectic temperature at 450°C and 436°C respectively. Mg has 0.16 nm atomic radius which is 12% larger than that of Al (0.143nm). Although addition of Mg in Al matrix, gives solid solution strengthening, i.e. Mg atoms are homogeneously distributed in Al matrix, but these atoms are prone to grain boundaries segregation [20] or surface segregation under different conditions which can severely affect performance of the alloy. The grain boundaries segregation could therefore relax some elastic strain which is due to their size effect, and hence stabilize the grain boundaries by reducing their energy [20]. But the extent of segregation has some correlation with grain boundary energy [21]. The equilibrium solubility limit of Mg in Al is less than 1 at.% at room temperature. Al with few at.% Mg alloy decomposes very slowly to form equilibrium precipitate Al_3Mg_2, as the phase has high nucleation barrier and hence grain boundaries play a crucial role in heterogeneous nucleation. Some studies indicate that the formation of Al_3Mg_2 (β) precipitates in binary Al-Mg alloy is through the GP zone [21] or metastable phase formation. $Solid\ Solution\ \alpha \rightarrow GP\ zones \rightarrow \beta'' \rightarrow \beta' \rightarrow \beta.$

Fe has very low solubility in Al, and in the presence of Mg, its solubility reduces further. The solubility of Mg in Al matrix is also reduced by the presence of Fe. Hence Fe (<0.4 wt.%) is mostly present as $FeAl_3/FeAl_6$ precipitates in Al-Mg binary alloy. Non-equilibrium solidification can lead to formation of Al_3Mg_2 phase even in Al-(2-3) wt.% Mg alloy along with large amount of Al_3Fe precipitates [22]. Fe can be present as Al_8Fe_2Si, Al_5FeSi or $FeMg_3Si_6Al_8$ if Si is present in Al-Mg alloy. This quartnary compound can form through the following invariant reaction in Al-Mg-Si-Fe system [22]. $L \rightarrow \ Al + Si + Mg_2Si + FeMg_3Si_6Al_8 \ \ at\ 554^{\circ}C.$

Presence of Si, enhance the probability of formation of Al-Mg_2Si low melting eutectic. When the concentration of these low melting phases is very less, the chances of solidification cracking are negligible. If these phases are present in large quantity, the likelihood of solidification cracking is again minimized as there is sufficient liquid to fill the gap created by the shrinkage cavities [18]. However, when these phases are present in the intermediate range, the probability of solidification cracking is the highest [21] which can be described by crack sensitivity curve of the Al-Mg or Al-Mg_2Si [23]. The peak of cracking sensitivity curve of Al-Mg system is at approximately 1.5 wt.% Mg and for Al-Si system, it is at 0.8 wt.% Si [23]. Thus Aluminum alloy containing more than 5.5 wt.% Mg or more than 3 to 4 % Mg_2Si phase have lower cracking probability than Al-2 wt.% Mg. To avoid solidification cracking during welding, this alloy is welded using Gas Tungsten Arc Welding (GTAW) process under high purity argon atmosphere and using 5356 grade aluminum weld wire as a filler wire. Although solidification cracking failure of the weld is minimized by this approach, the chances of HAZ liquation cracking still remain.

The reason behind HAZ liquation cracking is either melting of grain boundary eutectic phase in the HAZ or lower base metal solidus temperature than weld metal solidus. The mechanism of formation of low melting phase at HAZ is still unclear. It may be due to constitutional liquation or preferential grain boundary diffusion of alloying elements from the weld material [24, 25]. Constitutional liquation or localized liquation along the particle/matrix interface which contributes the HAZ liquation in alloys having second phase particles, is normally associated with the conventional welding process viz., GTAW, GMAW, SMAW [26] and presence of intermetallic particles at or above the eutectic temperature during heating is the prerequisite for constitutional liquation [27]. However, very rapid heating rate which is present in electron beam welding or laser welding, HAZ liquation cracking does not occur. Two schools of thought are there to describe the mechanism of HAZ liquation cracking. In one case, grain boundary penetration along with liquation of matrix particle play the key role in describing the cracking mechanism. Whereas in material which does not have any constituent particles, grain boundary segregation of impurity or solute elements explains the HAZ liquation cracking phenomena [26].

This paper deals with the analysis of two different failures observed in thin wall tube made of Al-2.1 wt.% Mg alloy. In one case, the port hole die extruded tube after several cold drawing and intermediate annealing failed during the hydro test. In another case, through-wall cracking is observed in the heat affected zone of the tube to tie-plate weld joint assembly. The results of investigation carried out using optical microscopy (OM) and scanning electron microscopy (SEM) with Energy Dispersive Spectrometry (EDS), Electron back scattered diffraction (EBSD) and micro-hardness measurement, to identify the cause of failures have been described.

2. In-homogeneity related cracking during pressure test of thin wall Al-2.1 wt.% Mg alloy tube.

The extruded tube made by port hole die extrusion process has 2.2 mm wall thickness. These tubes are subjected to a number of cold drawing steps with intermediate annealing at 475°C for 4 hrs. to achieve the final wall thickness of 1mm. The final stress relieving heat treatment is carried out at 200 °C for 1 hr. During cold drawing (Fig.1) as well as during hydro test some tubes were found to be fractured axially along a straight line.

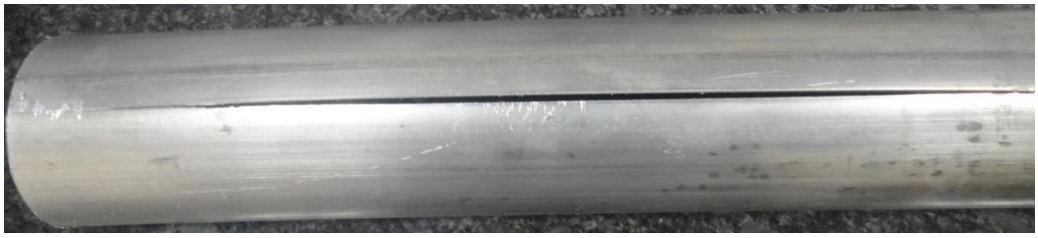

Fig. 1 Opening of port hole die extruded Al- 2.1 wt.% Mg tube along the seam.

One tube which failed in hydro-test, has been collected. The failed tube showed an axial crack of approximately 50 mm length. Fractography has been carried out on the cracked surface of this tube using SEM along with EDS analysis. Transverse section at the crack location has been prepared for microstructure

characterization. Different cross-sections of the tube away from the failure location are also prepared for microstructural investigation.

One sample from the tube, which qualified the hydro test at 250 psi, is also subjected to detailed investigation by metallography for the sake of comparison. The EBSD scans were carried out in LaB_6 CS3200L SEM fitted with a Nordlys MAX detector (HKL Technology A/S, Denmark) at 20 KV. The HKL Channel 5 software (HKL Technology A/S) was used for data analysis. In both the case after getting 1 μm surface finish in mechanical polishing, electro polishing has been carried out using an agitated solution of 10% perchloric acid, 90% ethanol at 20 V DC for approximately 30 sec. The temperature of the electrolyte has been maintained within 15-20°C during electro-polishing. Micro hardness measurements was carried out using 100 g load.

2.1 Optical Microscopy, Scanning Electron Microscopy with EBSD

The optical micrograph of the tube that passed the hydro test indicating presence of fine line along the joint is shown in Fig.2a. The higher magnification micrograph (Fig.2b) reveals the presence of etch-pits along the weld line. These pits are due to the piling up of dislocations along the weld joint which are revealed during etching. No cracks are observed in the optical micrograph. The EBSD inverse pole figure normal to the sample surface (IPF-Z) in the cubic stereographic projection of the transverse section of the flow tube shows crystallographic orientations of different grains [Fig. 2(c)]. The grains are slightly elongated along the tube circumferential direction with aspect ratio of approximately 2. A special CSL(Σ3) boundaries with misorientation 60° and CSL(13b) boundaries with misorientation 27.8 ° are also observed in the microstructure

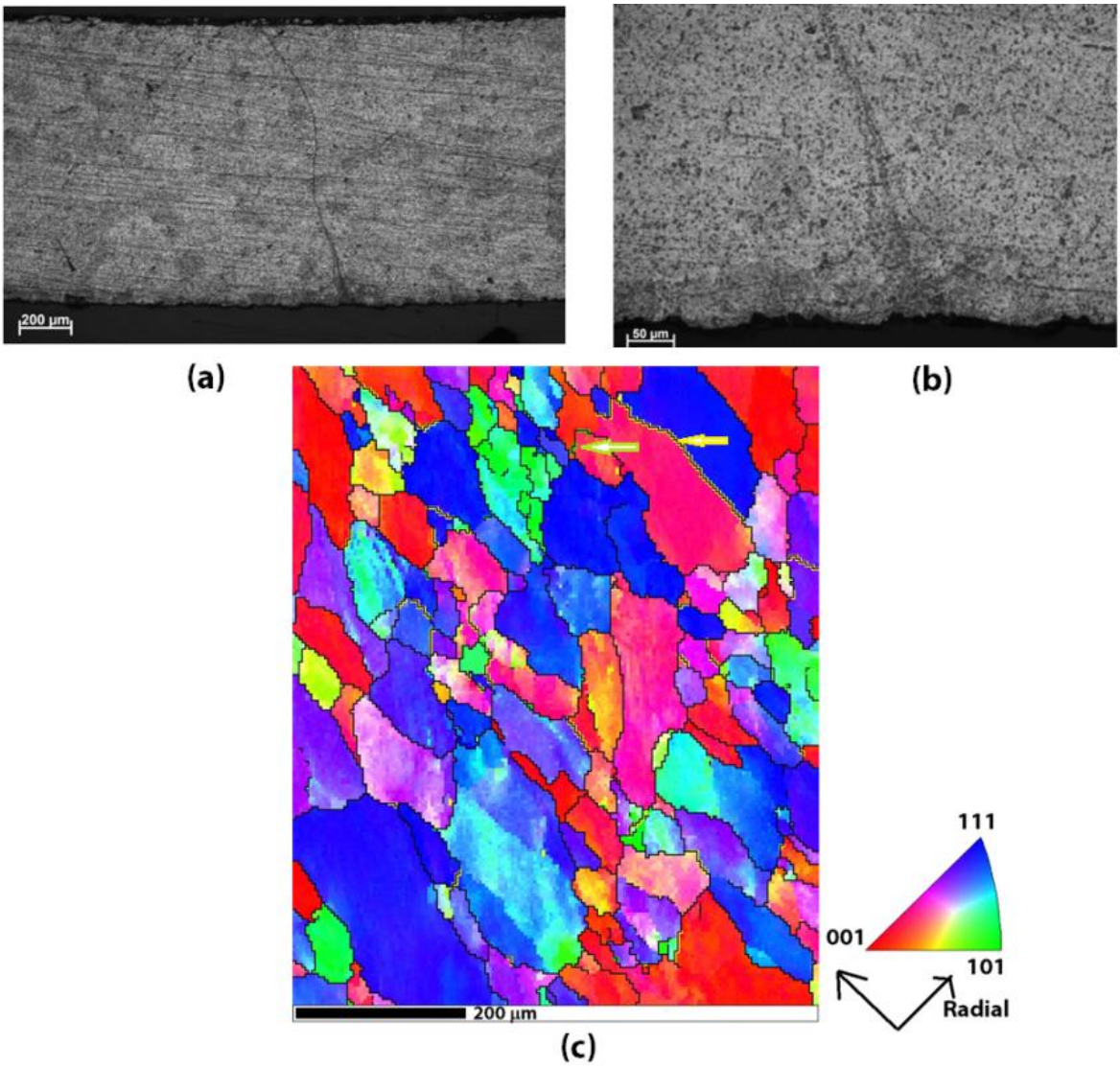

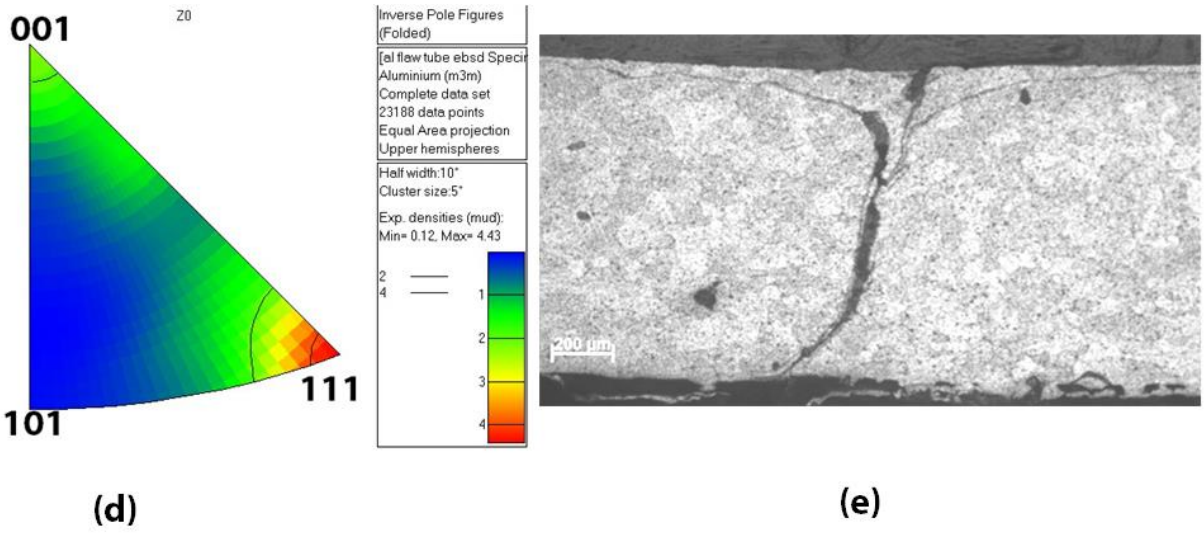

Fig. 2 (a) Optical micrograph of Al-2.1 wt.% Mg tube sample passed in hydro-test showing a very fine joint line was observed at low magnification, (b) High magnification optical micrograph of tube passed in hydro-test showing etch pits along the joint, (c) The orientation image as obtained from EBSD analysis of transverse section of Al-2.1 wt.% Mg tube. (The color code represents typical grain orientation along the z direction). The special CSLΣ3 (60°) and Σ13b (27.8°) boundaries are shown with yellow and green colored arrow, (d) The Inverse pole figure Z (surface normal) showing (111) major texture in final tube, (e) Optical microscope image of crack along the joint line in the transverse section of the tube.

which are found to be immune to grain boundary precipitation of β (Al_3Mg_2) [21] and hence should resist acid attack or intergranular corrosion [21]. The inverse pole figure (Fig.2d) normal to the surface indicates retention of deformation texture ([111] and [001]). The average hardness of the tube is HV 56.

The optical micrograph of the tube failed at the weld location (Fig.2e) shows the presence of crack along the weld line.

2.2 Fractography & EDS analysis

The fractured surface at the weld joint is seen in SEM (Fig.3a). Ploughing marks are seen on the surface, indicating metal flow in the extrusion direction. A higher magnification micrograph of the same surface is shown in Fig. 3b. The grains are flattened and nearly elongated in the direction of extrusion. No visible sign of gross deformation is evident from the fracture surface indicating easy separation at weld joint during the hydro test. The fracture surface is characterized by the presence of smooth features (Fig.3c) which indicates the presence of liquid at the time of fracture.

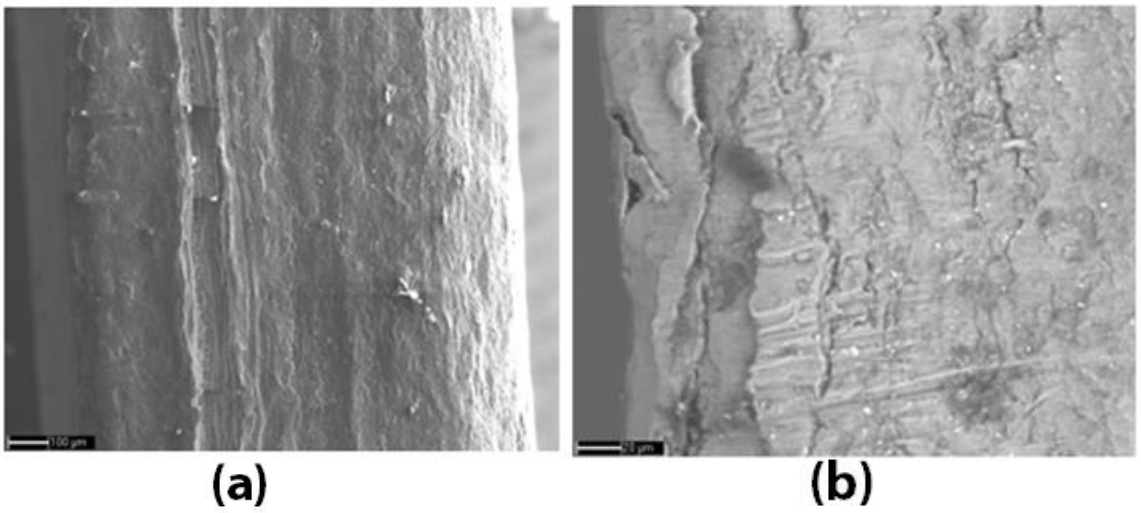

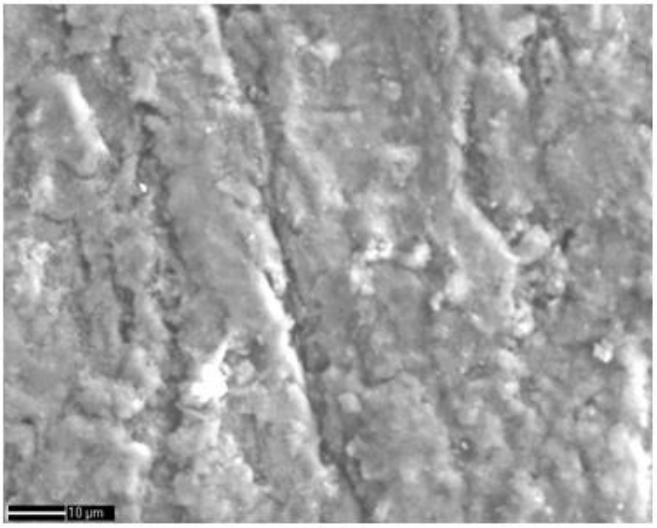

(c)

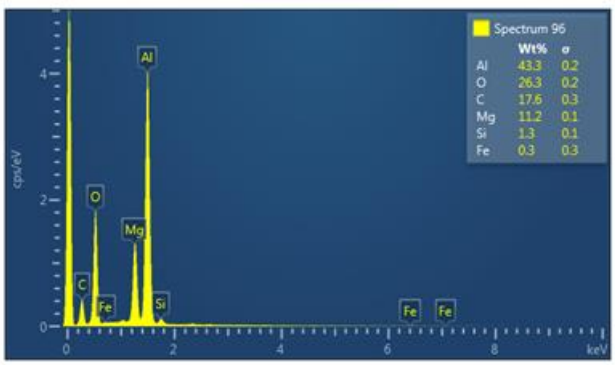

(d)

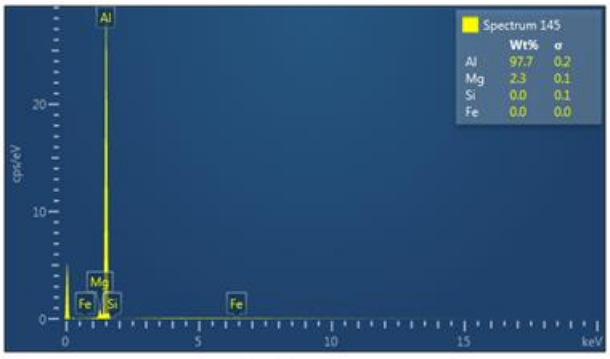

(e)

Fig 3. SEM micrographs of fracture surface at different magnification; a) ploughing mark indicating extrusion direction, b)Flat face appearance indicating no deformation, c) presence of liquid in the fracture surface as indicated by smooth appearance of fracture surface, d) EDS pattern at 10 KV from the fracture surface and (e) EDS pattern (at 20 KV) from the weld location of the tube which pass the hydro test.

The EDS pattern of the fractured surface (Fig. 3d) at low KV (10 KV) shows high concentration of Mg (8-19 wt.%) and Si(0.5-1.3 wt.%). The low accelerating voltage restricts the depth from which X rays are emitted, facilitates analysis of only the fracture surface region. The above ternary composition comprising of Al, Mg and Si has low solidus temperature around 500 to 530°C [22, 28] as compared to the solidus temperature of Al-2.1 wt.% Mg alloy (620°C). Hence, liquation of the regions having this ternary constituent at the weld joint area is possible during fabrication, when there is localized adiabatic heating [29] and separation occurs along this region under the presence of tensile stresses. The fracture surface also shows a high oxygen content. This may be due to the formation of oxide after fracture as the fractured aluminum surface spontaneously undergoes oxidation. The fracture surface also has high C. This C contamination may occur during handling or due to the trapped residual lubricant Accurate determination of C in SEM is beyond the scope of SEM. Fig. 3e shows the EDS pattern of the tube at the weld location, which passed the hydro test. Contrary to the observations on the failed tube, this tube does not show high concentration of Mg (2.3 wt.%) and Si in the weld region.

2.3 Cause of failure

Weldability during porthole extrusion is influenced by a number of factors such as: (i) the die design, (ii) the lubricant, (iii) the billet temperature and (iv) the extrusion speed. If the lubrication is not proper, it may contaminate the joining surfaces leading to improper welding. High billet temperature may lead to incipient

melting at weld joint resulting in poor weld quality. Similarly, high extrusion speed can alter the temperature of the extrudate leading to the formation of improper weld.

From the investigations carried out it can be concluded that during port hole die extrusion process, Mg and Si rich continuous low melting metastable/equilibrium phase formation occur along the weld line due to high billet temperature and extrusion speed. Presence of low melting phase along the weld line during processing lead to formation of micro-cracks and poor quality weld joint. These micro cracks could have grown during further processing or during hydro test leading to the failure of the tube along the weld joint. The complete decoration of the weld joint with Mg, Si rich phase supports this hypothesis. The cracks gets arrested in the ductile aluminum matrix if the precipitation is not continuous.

2.4 Remedial Measure

Proper control of billet temperature and extrusion speed is utmost necessary to avoid such cracking.

3. HAZ liquation cracking of Al-2.1 wt.% Mg tube and the tie-plate weld assembly.

A through-wall crack is observed in the heat affected zone of the welded Al-2.1 wt.% Mg tube and tie plate assembly (Fig.4 a, b). The welding is carried out by gas tungsten arc welding (GTAW) using 2.4 mm dia. 5356 grade aluminum electrode.

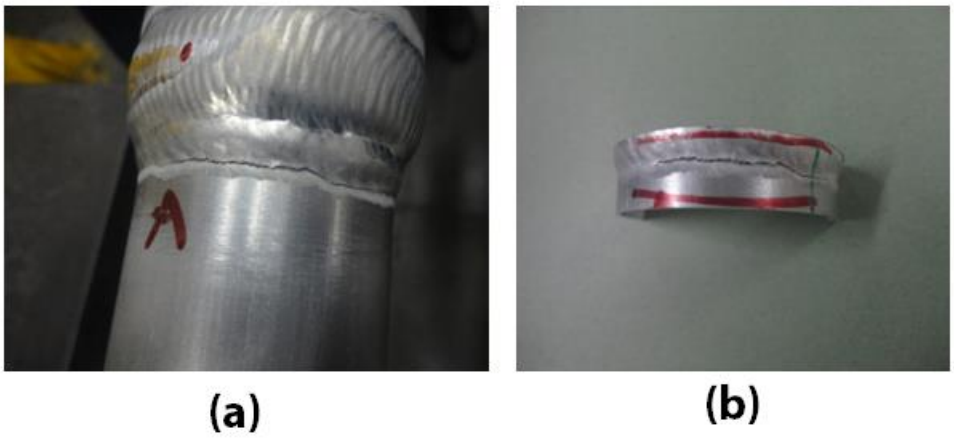

Fig 4. (a) Failure location; crack was found on the weld-parent metal interface (b) cut sample taken from for failure analysis

The chemical composition of the tube material and the electrodes are given in Table 1 and 2 respectively. The electrode contains more than 5 wt. % Mg to avoid weld solidification cracking. Samples comprising of weld, HAZ and parent metal are taken from the crack location for detailed investigations involving optical microscopy, scanning electron microscopy with EDS and EBSD and micro-hardness measurement. A sample from the weld joint in the acceptable tube is also investigated for the sake of comparison.

Table 1: Chemical composition in wt.% of the Al-2.1 wt.% Mg tubes used in GTA welding

Si	Cr	Mg	Cu	Fe	Mn	Zn	Al
0.157	0.031	2.12	0.008	0.13	0.013	0.001	Balance

Table 2: Chemical composition of filler wire (wt.%) used for GTA welding of Al-2.1 wt.% Mg tube with tie plate

Si	Cr	Mg	Cu	Fe	Ti	Zn	Al
0.011	0.072	5.14	0.021	0.13	0.08	0.022	Balance

3.1 Optical microscopy, SEM, EDS and EBSD analysis

The optical micrograph of the transverse section at the crack location is shown in Fig.5 a and b. The micrograph shows that the nature of the crack is intergranular. The SEM micrograph of the heat affected zone in

the etched condition is shown in Fig.5c. It shows the presence of precipitates at the grain boundary near the cracked surface. As one moves towards the base metal, the extent of precipitate decoration at the grain boundaries reduces. The micro-hardness profile across the weld, HAZ and base metal indicates peak hardness at the HAZ location, just near weld (HV 60) and EDS analysis indicates Mg concentration of approximately 2.4 wt.% in the HAZ.

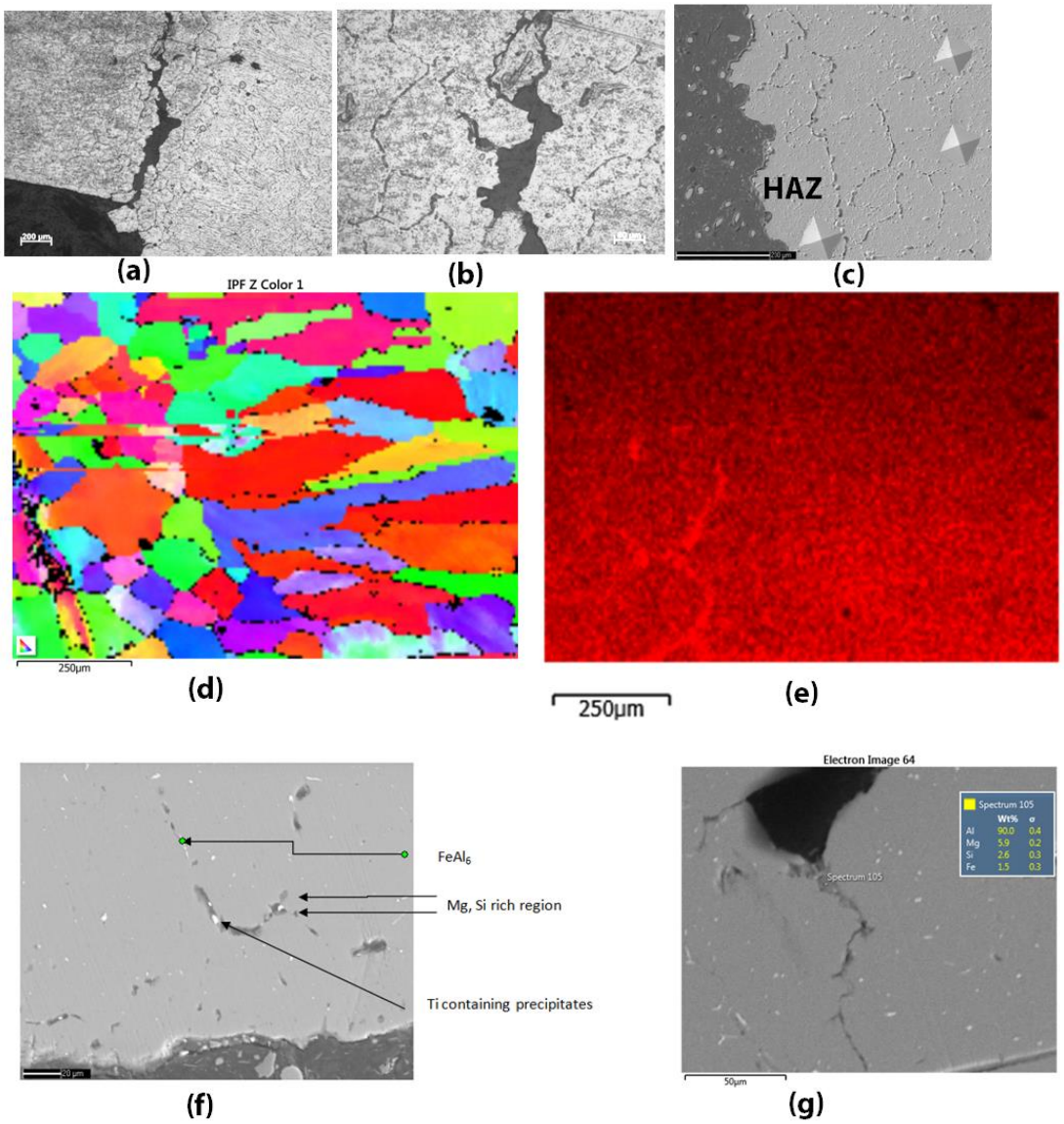

Fig 5. (a) Optical Micrograph of cracked weld assembly of Al-2.1 wt.% Mg alloy indicates presence of cracks at HAZ location and (b) Higher magnification image indicates Intergranular nature of the crack, (c) SEM micrograph of HAZ region after etching showing grain boundary decoration, extent of decoration reduces towards base metal (d) Inverse pole figure map (IPF-Z) obtained from EBSD at transverse section of good Al-2.1 wt.% Mg tube tie plate weld joint. (The color code represents orientation of grains along the z direction), the black dot regions are of second phase precipitates which are mostly present at grain boundaries (e) The Mg Kα1_2 image mapping obtained from same location using EDS indicates Mg rich region at the grain boundary just at the HAZ location near weld (f) SEM BSE image of some micro-cracks along with different phases, (g) High magnification BSE image of tight portion of the crack having high amount of Mg, Si, Fe rich phase.

Figure 5d shows the results of EBSD analysis of a weld sample, which did not reveal through and through cracking. The EBSD inverse pole figure normal to the sample surface (IPF-Z) in the cubic stereographic projection of the transverse section of the weld between the thin tube and tie-plate shows crystallographic

orientations of different grains at the weld and HAZ regions (Fig.5.d). The columnar grain structure with aspect ratio 5 in the weld along with the presence of black spot (un-indexed) at grain boundaries which are mostly from second phase precipitates are seen. Presence of the grain boundary decoration with the black spot is significant at HAZ location. The grains at the HAZ locations are equiaxed and coarse. The simultaneous EDS count indicates that the grain boundaries of HAZ region are rich in Mg (Fig.5e), although complete decoration of grain boundaries with precipitates is absent in the good weld.

SEM micrographs of the as-polished cracked sample in the backscattered mode are given in Fig.5 f-g. The micrograph (Fig. 5f) indicates presence of precipitates of different morphologies, some appear dull whereas others are bright colored and needle shaped in back scattered mode. SEM micrograph of tight crack along with the results of EDS analysis for the second phase precipitates present within the micro crack is given in Fig.5g. The result indicates that the precipitates are rich in Mg (6 wt. %), Si (2.6 wt. %) and Fe (1.5 wt.%).

The morphology of typical grain boundary film which are rich in Mg are given in fig.6a. These film are associated to micro-cracks. EDS analysis of the needle shaped bright colour precipitate and the dull precipitate within the crack (Fig.6b), are given in Fig.6 c and Fig.6d respectively. The results of EDS analysis for the matrix near the crack location indicates Mg, in the range of 2.1 to 2.7 wt. % . The EDS result of needle shape bright colour precipitate shows that these precipitates are rich in Fe (10 to 25 wt.%) with some amount of Mg (2 to 2.8 wt.%) and Si (0.2 wt.%). From the morphology and the EDS analysis, these needle shaped precipitates are found to be of $FeAl_6$ [30]. The EDS analysis (Fig.6d) for the dull phase present within the crack shows that the phase is rich in Mg (3 to 6 wt.%) and Si (3 to 7 wt.%) with some amount of Fe (1 to 2 wt.%).

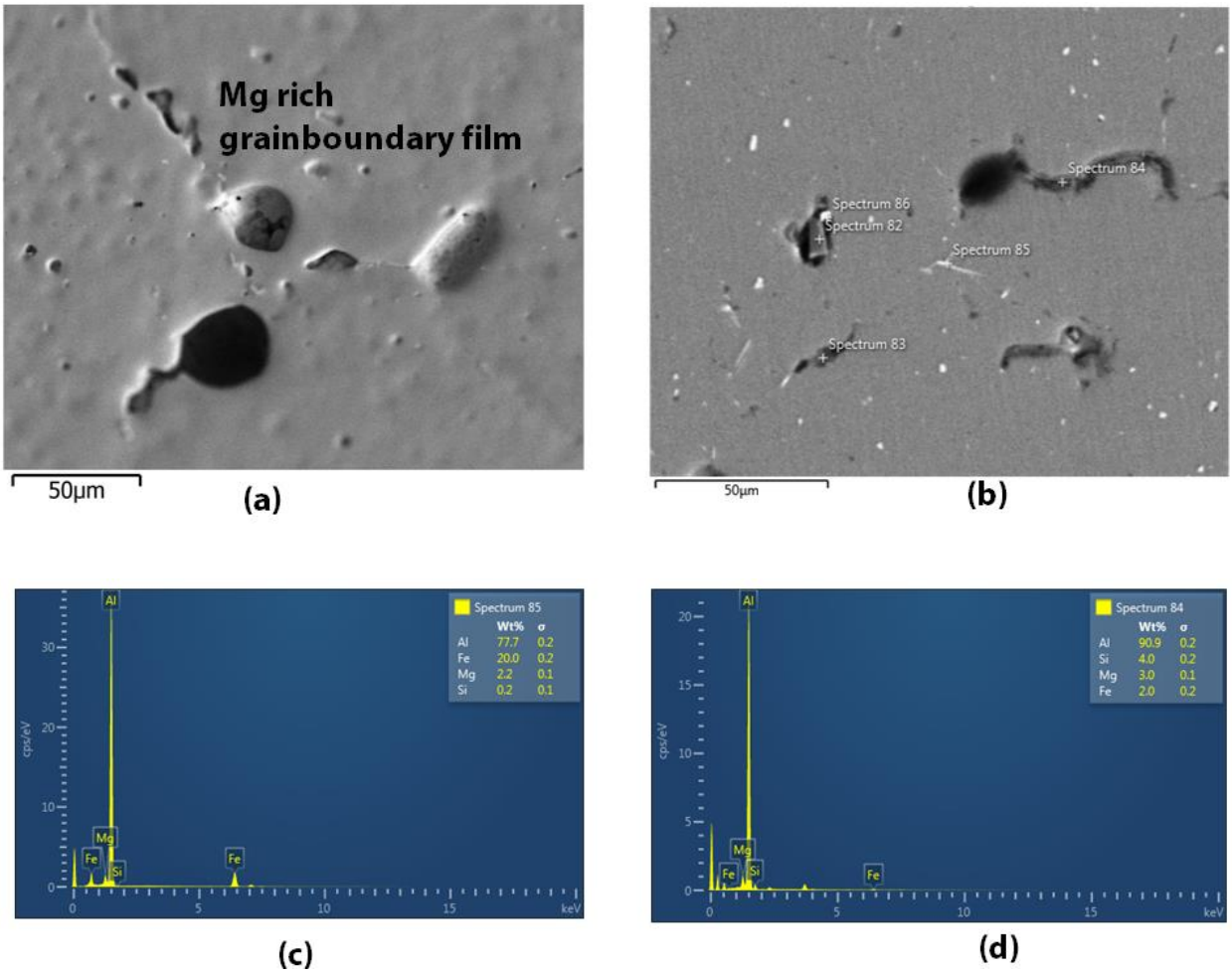

Fig.6(a) SEM image of grain boundary film, (b) BSE image of as polished sample showing presence of different morphology of precipitates, (c) EDS analysis needle shape bright phase, (d) EDS analysis at the dull phase present at crack.

3.2 Fractography

The crack face is observed under scanning electron microscope. The fracture surface (Fig.7) shows intergranular appearance and is characterized by the presence of smooth features, which indicates the presence of liquid at the time of fracture. The tip of the grains that are exposed to the fracture surface have 'egg-crate' appearance, which is typical of intergranular fracture. Table 3 shows the results of the EDS analysis carried out at 10 KV at the fractured surface and at 20 KV at the base metal. The table indicates that the fractured surface contains significantly higher concentration of Mg, Si and Fe as compared to the base metal.

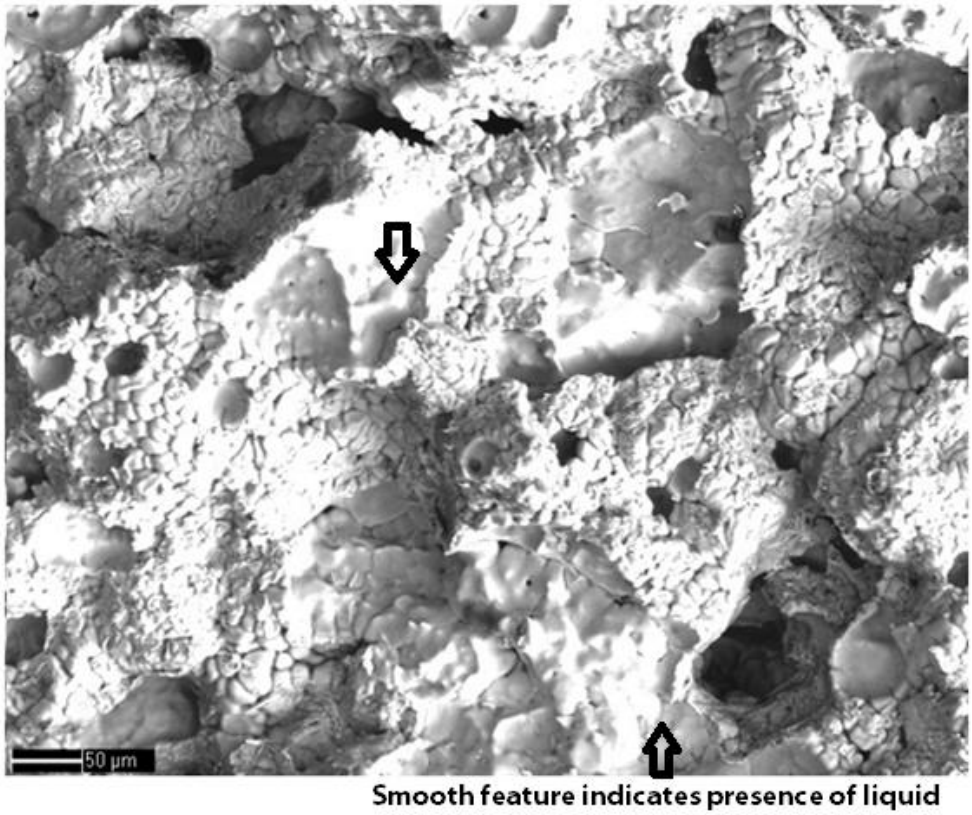

Fig. 7: Intergranular appearance of cracked face, seen under SEM

Table 3 : EDS analysis at different accelerating voltage on fracture surface and at matrix away from crack

	Fracture Surface	Away from crack
Accelerating voltage	10 KV	20 KV
Mg (wt.%)	8.1	2.3
Si (wt.%)	1.2	0.1
Fe(wt.%)	1.8	0.2
Al (wt.%)	Balance	Balance

3.3 Cause of failure

Based on the results of the above investigations, it can be concluded that the low melting metastable phase comprising of Mg, Si and Fe was present at the grain boundary in the HAZ region. Fe is partitioned in the grain-boundary phase as it has poor solubility in Aluminium. It is also present as $FeAl_6$ within the grains. During welding, Mg from weld or matrix of HAZ, diffuse towards the grain boundaries and form low melting constituent. These grain-boundary precipitates grow like allotriomorphs under the influence of welding heat just near the weld region and decorate the entire grain boundaries. When the temperature in the HAZ just near fusion line reaches the liquidus temperature of the grain-boundary precipitate (during welding), liquation at the grain

boundary occurs because of the presence of low melting phase. However, the grains at the HAZ location are still in the solid state. During cooling, due to the presence of mechanically or thermally induced restraint, grains are separated along the grain boundary as the liquid film cannot withstand the tensile stresses. This leads to the formation of a crack in the heat affected zone.

3.4 Remedial Measure

Since tensile stress is necessary to cause cracking, it may be possible to avoid cracking with susceptible material by adapting the procedures which ensure presence of compressive stress at HAZ during welding.

4. Conclusion.

The failure analysis carried out on two tubes made of Al-2.1 wt.% Mg, one of which failed during the hydro test and the other after welding to the tie-plate, revealed that in both the cases presence of low melting stable/metastable phase of Al-Mg-Si is responsible for the failures. In the case of tube failing during the hydro test, segregation of Mg and Si at the weld-line during the port hole extrusion process led to the formation of low solidus alloy composition and micro cracking. These micro-cracks grew during subsequent processing and leading to failure during hydro test. In the second case, the complete decoration of Al-Mg-Si-Fe rich phase at the grain boundary in the HAZ region resulted in liquation of the grain boundaries during welding, leading to cracking under tensile stress during cooling.

5. References

[1] Rajiv Sikand, Arun M Kumar, Anil K Sachdev, Alan A Luo, Vipin Jain, Anil K Gupta, AM30 porthole die extrusions—A comparison with circular seamless extruded tubes, J. Mater. Process. Technol. 209 (2009) 6010–6020.

[2] M K Malik, Manufacture of aluminum alloy components for nuclear applications, Proceedings of National Symposium on Manufacture of Nuclear Components, April 7-8,1982, BARC, Mumbai, M12-1-M12-17.

[3] Akaret R, Extrusion welds-quality aspects are now center stage, *Proceedings of the 5th International Aluminum Extrusion Technology Seminar Papers*, Chicago, 1992, 319-336.

[4] Plate M and Piwnik J, Theoretical and experimental analysis of seam weld formation in hot extrusion of aluminum alloys, *Proceedings of 7th International Aluminum Extrusion Technology Seminar*, Chicago, 2000, Vol.1, 205-211.

[5] Bourqui B, Huber A, Moulin C, A Bunetti Improved weld seam quality using 3D FEM simulation in correlation with practice, *The first EAA extrusders division congress*, Brescia Italy, 2002.

[6] Jo H H, Jeong C S, Lee S K, B M Kim, Determination of welding pressure in the non steady-state porthole die extrusion of improved Al7003 hollow section tubes, J. Mater. Process. Technol. 2003, 139 (1-3), 428-433.

[7] Fazzini P A B and Bellotti S, How to obtain quality profiles surfaces. *Aluminio E Leghe* 2008, 6, 81-85.

[8] Donati L and Tomesani L, The effect of die design on the production and seam weld quality of extruded aluminum profiles, J. Mater. Process. Technol. 2005 (164-165) 1025-1031.

[9] Ceretti E, Fratini L, Gagliardi F, C. Giardini , A new approach to study material bonding in extrusion porthole die, *CIRP Annals Manufacturing Technol.2009*, 58(1), 259-262.

[10] Bingöl S, Keskin, M S and Bozaci A, Properties of seam welds produced with different extrusion parameters, *Arch. Mater. Sci. Eng.* 2007, 28(6), 365- 368.

[11] Bingol S and Keskin M S, Effect of different extrusion temperature and speed on extrusion welds, J. Achiev. Mater. Manuf. Eng. 2007, 23(2), 39-42.

[12] Zhang C S, Zhao G Q, Chen Z R, *H Chen, F J Kou*, Effect of extrusion stem speed on extrusion process for a hollow aluminum profile, *Mater. Sci. and Eng. B - Adv. Functional Solid State Materials 2012*, 177, 1691-1697.

[13] Den Bakkera J A, Werkhoven R J, Sillekens W H, Katgerman L, The origin of weld seam defects related to metal flow in the hot extrusion alloys EN AW-6060 and EN AW-6082, J. Mater. Process. Technol. 2014, 214, 2349–2358.

[14] Valberg H, Loeken T, Hval M, Nyhus B, Thaulow C, The extrusion of hollow profiles with a gas pocket behind the bridge, Int. J. Mater. Prod. Technol. 1995, 10(3-6), 222–267.

[15] Donati L, Tomesani L, The effect of die design on the production and seam weld quality of extruded aluminum profiles, J. Mater. Process. Technol. 2005, 164, 1025–1031.

[16] Kim K J, Lee C H , Yang D Y, Investigation into the improvement of welding strength in three-dimensional extrusion of tubes using porthole dies, J. Mater. Process. Technol. 2002, 130, 426–431.

[17] Zhang Y M, Pan C, Male A T, Solidification behavior of Al–Mg aluminum alloy using double-sided arc welding process, J. Mater. Sci. Lett. 2000;19, 831–833.
[18] Dickerson PB, Welding of aluminum alloys. Welding, brazing and soldering, ASM metals handbook, vol. 6. Metals Park, Ohio: ASM international; 1993, 722–729.
[19] J H Dudas and F R Collins, Preventing Weld Cracks in High-Strength Aluminum Alloys, Weld. J., 1966, 45, 241s-249s.
[20] X Sauvage, N Enikeev, R Valiev, Y Nasedkina, M Murashkin, Atomic-scale analysis of the segregation and precipitation mechanisms in a severely deformed Al–Mg alloy, Acta Materialia, 15 June 2014, 72, 125-136.
[21] Jianfeng Yan, Nathan M Heckman, Leonardo Velasco and Andrea M Hodge, Improve sensitization and corrosion resistance of an Al-Mg alloy by optimization of grain boundaries, www.nature.com/scientificreports/ScientificReports, 6:26870, DOI: 10.1038/srep26870.
[22] Nikolay A Belov, Dmitry G Eskin and Andrey A Aksenov, Chapter 2 - Alloys of the Al−Mg−Si−Fe System, Multicomponent Phase Diagrams Applications for Commercial Aluminum Alloys, ISBN: 978-0-08-044537-3, Copyright © 2005 Elsevier Ltd. http://www.sciencedirect.com/science/book/9780080445373, Pages 47-82.
[23]file:///home/internetuser/Desktop/Downloads/How%20to%20Avoid%20Cracking%20in%20Aluminum%20Alloys.html
[24] N F Gittos, M. H Scott, Heat-Affected Zone Cracking of Al-Mg-Si Alloys**,** Welding Research Supplement to the welding Journal, June 1981, 60(6), 95-103.
[25] M Katoh, H W Kerr, Investigation of Heat-Affected Zone Cracking of GTA Welds of Al-Mg-Si Alloys Using the Varestraint Test, Welding Research Supplement, December 1987, 360-368.
[26] Lippold J C, I I I Baeslack W A and Varol I, Heat-affected zone liquation cracking in austenitic and duplex stainless steels, Welding Research Supplement, January 1992, 1s-14s.
[27] Ojo O A, Richards N L, Chaturvedi M C, Contribution of constitutional liquation of gamma prime precipitate to weld HAZ cracking of cast Inconel 738 superalloy, Scripta Materialia, (2004), 50, 641–646.
[28] M F Gittos, Welding Al-Mg-Si alloy, The welding Institute Research Bulletin, July 1986, 27, 230-235.
[29] V V ZAKHAROV, Scientific aspects of deformability of aluminium alloys during extrusion, Adv Perform Mater., 1995, 2, 51- 66.
[30] Lifeng Zhang, Jianwei Gao, Lucas Nana Wiredu Damoah, and David G Robertson, Removal of iron from aluminum: a review, Miner. Process. Extr. Metall. Rev., 2012, 33, 99–157.